The Journal of Navigation (2021), **74**:3 698–712
doi:10.1017/S0373463321000035

RESEARCH ARTICLE

Analysis of impact of group delay on slope distortion of S-curve in delay locked loop

Yuqi Liu,* Yihang Ran, Yi Yang, Lin Chen, Tuling Xiong, and Hongchen Pan

The 29th Research Institute of China Electronics Technology Group Corporation, Chengdu, China.
*Corresponding author. E-mail: liu.yuqi@139.com

Received: 12 August 2020; **Accepted:** 10 January 2021; **First published online:** 9 February 2021

Keywords: delay locked loop, satellite navigation, signal processing, spread spectrum, tracking loop

Abstract

As essential specifications of correlation domain for signal quality evaluation, distortions of the S-curve, including bias and slope distortions of the zero-crossing point, are usually selected as indicators of optimisation in the process of designing the channels of receivers or navigation satellites. Focusing on this issue, we present a detailed analysis of slope distortion in the presence of group delay and amplitude distortions. After validating the theoretical results, we present further discussions about the impacts of different group delay terms on slope distortions. The results indicate that both the odd-order and the even-order terms have impacts on the slope distortion, and higher odd-order terms have less slope distortion compared with the lower odd-order terms. These results are useful for evaluating the slope distortion from the group delay and guiding improvement in design of the channel.

1. Introduction

The wide use of satellite navigation in various fields has dramatically increased the demand for more precise positioning performance. Several satellite navigation systems continue to improve their service accuracy (Thoelert et al., 2019; Yang et al., 2019; Wu et al., 2020; Yang et al., 2020). Most attention in recent years has been paid to the scope of modelling and evaluating the errors that cause degradation of positioning performance, derived from satellite navigation payloads and receivers. For precision positioning, the signal should be broadcast from the satellite with limited distortion and passed through the high fidelity channel of the receiver. Thus, to reduce the degradation of performance, we should model and optimise the channels during design.

Numerous signal quality evaluations for broadcast navigation signals and analyses of the impact of RF (Radio Frequency) channel distortions on signal quality have been performed (Betz, 2002; Soellner et al., 2002; Gu et al., 2014; Quan et al., 2015; Liu et al., 2019). Notably, some correlation domain indicators, such as S-curve bias, slope distortion of S-curve and correlation loss, are usually selected as the targets of optimising the channel or as the indicators for evaluating the quality of the broadcast signal.

The standard deviation of the code tracking error is an important indicator for code tracking and is directly related to the positioning performance. The code tracking loop, also termed delay locked loop (DLL), is implemented by early-minus-later processing. In the processing, the discriminator curve is obtained by further combining the correlation functions calculated between the replica code and the received signal. To attain the desired loop performance, the shape of the correlation function should be as close to the ideal case as possible. Prior results from Betz (2002) show that the standard deviation of code tracking error is proportional to the loop bandwidth, and the loop bandwidth

is inversely proportional to the discriminator gain that depends on the S-curve slope. Any distortions in the slope of the S-curve would cause the code tracking loop to deviate from the expected behaviour.

Warner and Last (2009) presented an explanation of the discriminator curve and the sign of the tracking error. Focusing on the non-ideal distortion of the group delay from the ionosphere, Guo et al. (2014) performed analysis of the S-curve bias for the Galileo E5 signal (European Union, 2013). He et al. (2020) evaluated the S-curve biases of BDS (BeiDou Navigation Satellite System) signals from the sampled data using a 40 m dish antenna. B1I and B3I of BDS were selected as examples to be analysed, considering different parameter configurations of receivers. Some suggestions about choosing proper correlator spacing and bandwidth were provided. Liu et al. (2020) investigated the phase bias among the signal components modulated on the same centre frequency and revealed that the components having different types of modulation are more sensitive to the phase bias. Pseudo-range bias, which is directly related to S-curve bias, was evaluated using measurements extracted from the receiver (Hauschild and Montenbruck, 2016; Gong et al., 2018). These researches reveal that the bias is strongly related to the receiver configuration. The authors (Liu et al. 2019) presented the model of the bias of the S-curve affected by the group delay. By expanding the group delay in the Taylor form (Zhu et al., 2009) with different order terms, we revealed the mechanism of the bias of S-curve from the group delay. Based on these previous works, we can see that the bias of the S-curve is affected by the receiver's different configurations. It would bring unpredicted biases into the pseudo-range measurements for different types of receivers.

Betz and Kolodziejski (2009a, 2009b) presented the analytic model of the loop performance for DLL. Their results show that the slope of the S-curve is a part of the denominator of the tracking error expression of the code tracking loop. Without including the distortion of group delay, Liu et al. (2012) analysed the slope of the discriminator curve in the case of only considering the band-limited effect. The slope distortion was evaluated using a numerical method (Soellner et al., 2002; Xie et al., 2018). The slope distortion of the S-curve and other indicators of signal quality were defined and analysed in the presence of group delay distortion by Betz (2002). The results show that the non-ideal RF channel would change the discriminator's slope. Once the group delay's effect is included in the model, the corresponding bias of the S-curve has to be handled properly before performing further calculation of slope distortion. Focusing on this issue, we present a detailed analysis of S-curve slope distortion due to the non-ideal group delay, and analyse slope distortions for different types of group delay containing different order terms. The presented results can be used for improving the channel design for navigation payloads or receivers.

The content of the paper is as follows: first, the model of the slope distortion from the group delay is provided; the theoretical analysis is then validated by the simulation; third, the slope distortions for different cases of group delay are further analysed in detail. Finally, conclusions about the impact of group delay on slope distortion are made.

2. Model of slope distortion

Filters are important in the transmitting channels of payloads and receiving channels of receivers. For the transmitting channel, the filter is responsible for filtering the out-band part of the transmitted signal. And for the receiving channel, the filters are used for blocking the adjacent out-band signal into the channel. In engineering practice, their bandwidths are usually limited, and their amplitude and group delay usually show an inevitable fluctuation within the bandwidth. The control of the amplitude fluctuation is more accessible compared with that for group delay.

In the model, the received signal $c^f(t)$ denotes the signal $c(t)$ filtered with the frequency response of $h(t)$. The equivalent baseband signal containing $c^f(t)$ is processed in the DLL of the receiver using an early-minus-late power discriminator algorithm. It is noted that the method presented here can also be applied to analyse slope distortion for other types of discriminator algorithms. Then, the discriminator

https://doi.org/10.1017/S0373463321000035 Published online by Cambridge University Press

output is given by Liu et al. (2019)

$$\mathrm{D}_{EMLP}(\tilde{\tau}) = \mathrm{R}\left(\tilde{\tau} - \frac{d}{2}T_c\right) * \mathrm{R}^*\left(\tilde{\tau} - \frac{d}{2}T_c\right) - \mathrm{R}\left(\tilde{\tau} + \frac{d}{2}T_c\right) * \mathrm{R}^*\left(\tilde{\tau} + \frac{d}{2}T_c\right) \tag{1}$$

where d is the correlator spacing; T_c is the pseudorandom code rate; and $R(\tilde{\tau})$ is given by

$$R(\tilde{\tau}) = \sqrt{2P}e^{\mathrm{i}\varphi_0}\int_{-B_f/2}^{B_f/2} P(f)H(f)e^{\mathrm{i}2\pi f\tilde{\tau}}\mathrm{d}f \tag{2}$$

where $P(f)$ means the signal's power spectral density; B_f is the bandwidth limited by the front-end of the receiver; $H(f)$ denotes the equivalent filter of the channel and can be further written as $A_a(f)e^{\mathrm{i}*\theta(f)}$; and φ_0 is the initial carrier phase.

According to the theory of tracking loop (Betz, 2002; Kaplan and Hegarty, 2006), $D_{EMLP}(\tilde{\tau})$ is zero when the loop locks. Assume that τ_r is the delay of the maximum peak correlation between the received and replica signals, then $D_{EMLP}(\tau_r, d) = 0$ as long as the channel is ideal. Once the non-ideal property is introduced, a correlator spacing related bias $\delta\tau$ would exist to satisfy $D_{EMLP}(\tilde{\tau}, d) = 0$, where $\tilde{\tau} = \tau_r + \delta\tau$. Thus, the slope of the S-curve can be written as

$$K_{\mathrm{EMLP}}(d) = D'_{EMLP}(\tilde{\tau}, d)|_{\tilde{\tau}=\tau_r+\delta\tau} \tag{3}$$

where $\mathrm{D}'_{EMLP}(\tilde{\tau}, d) = \mathrm{d}D_{EMLP}(\tilde{\tau}, d)/\mathrm{d}\tilde{\tau}$. Using a similar method to that in Liu et al. (2019), τ_r can be expressed as the terms of the zeroth-order of the group delay plus a constant $\Delta\tau$, that is

$$\tau_r = \tau_g + \Delta\tau \tag{4}$$

where $\Delta\tau = -\mathrm{R}'_s(\tilde{\tau})/\mathrm{R}''_s(\tilde{\tau})|_{\tilde{\tau}=\tau_g}$ and $R_s(\tilde{\tau}) = 2P\int_{-B_f/2}^{B_f/2} P(f)H(f)e^{\mathrm{i}2\pi f\tilde{\tau}}df\int_{-B_f/2}^{B_f/2} P(f)H(f)e^{-\mathrm{i}2\pi f\tilde{\tau}}df$.

Further $\delta\tau(d)$ can be calculated by

$$\delta\tau(d) = -\frac{D_{EMLP}(\tau_r, d)}{D'_{EMLP}(\tau_r, d)} \tag{5}$$

Substituting Equation (2) into (3) yields

$$\begin{aligned} K_{\mathrm{EMLP}}(d) = {} & 2P\mathrm{i}\pi\int_{-B_f/2}^{B_f/2} fP(f)A_a(f)e^{\mathrm{i}\theta(f)}e^{\mathrm{i}2\pi f\left(\tilde{\tau}-\frac{d}{2}T_c\right)}\mathrm{d}f \\ & \times\int_{-B_f/2}^{B_f/2} P(f)A_a(f)e^{-\mathrm{i}\theta(f)}e^{-\mathrm{i}2\pi f\left(\tilde{\tau}-\frac{d}{2}T_c\right)}\mathrm{d}f \\ & - 2P\mathrm{i}\pi\int_{-B_f/2}^{B_f/2} fP(f)A_a(f)e^{-\mathrm{i}\theta(f)}e^{-\mathrm{i}2\pi f\left(\tilde{\tau}-\frac{d}{2}T_c\right)}\mathrm{d}f \\ & \times\int_{-B_f/2}^{B_f/2} P(f)A_a(f)e^{\mathrm{i}\theta(f)}e^{\mathrm{i}2\pi f\left(\tilde{\tau}-\frac{d}{2}T_c\right)}\mathrm{d}f \end{aligned}$$

https://doi.org/10.1017/S0373463321000035 Published online by Cambridge University Press

$$
\begin{aligned}
&-2Pi\pi\int_{-B_f/2}^{B_f/2} fP(f)A_a(f)e^{i\theta(f)}e^{i2\pi f\left(\tilde{\tau}+\frac{d}{2}T_c\right)}\mathrm{d}f\\
&\times\int_{-B_f/2}^{B_f/2} P(f)A_a(f)e^{-i\theta(f)}e^{-i2\pi f\left(\tilde{\tau}+\frac{d}{2}T_c\right)}\mathrm{d}f\\
&+2Pi\pi\int_{-B_f/2}^{B_f/2} fP(f)A_a(f)e^{-i\theta(f)}e^{-i2\pi f\left(\tilde{\tau}+\frac{d}{2}T_c\right)}\mathrm{d}f\\
&\times\int_{-B_f/2}^{B_f/2} P(f)A_a(f)e^{i\theta(f)}e^{i2\pi f\left(\tilde{\tau}+\frac{d}{2}T_c\right)}\mathrm{d}f
\end{aligned}
\tag{6}
$$

where $\theta(f)$ is

$$
\theta(f)=\theta_0-2\pi\tau_g f-\frac{1}{2}(2\pi)^2\tau_{g1}f^2-\frac{1}{6}(2\pi)^3\tau_{g2}f^3-\frac{1}{24}(2\pi)^4\tau_{g3}f^4 \tag{7}
$$

The slope distortion of the S-curve is defined as the ratio between the distorted and ideal slopes (Betz, 2002), and its logarithmic form is given by

$$
K_{sd}(d)=20*\mathrm{LOG}\left(\frac{K_{\mathrm{EMLP}}(d)}{K_{\mathrm{EMLP}}^{\mathrm{ideal}}(d)}\right) \tag{8}
$$

According to the model in the references, the standard deviation of code tracking error is inversely proportional to $K_{\mathrm{EMLP}}(d)$ (Betz and Kolodziejski, 2009a, 2009b). In practice, the loop design should meet the demand for dynamics, tracking error, etc. The existence of distortion on the slope of the S-curve would cause the tracking loop to deviate from the expected behaviour.

3. Validation

In this section, the theoretical analysis is validated by the simulation. The group delay in the simulation is derived from the model (Liu et al., 2019), and the corresponding curve is plotted in Figure 1. The coefficients of different order terms in the model are given as follows: $\tau_g = 23\cdot 5\mathrm{E}-9$ (s); $\tau_{g1} = 1\cdot 8\mathrm{E}-17$ ($\mathrm{s}^2/\mathrm{rad}$); $\tau_{g2} = 1\cdot 75\mathrm{E}-24$ ($\mathrm{s}^3/\mathrm{rad}^2$); and $\tau_{g3} = 4\cdot 2\mathrm{E}-33$($\mathrm{s}^4/\mathrm{rad}^3$).

Here, we select BPSK(10) as an example to be analysed. The GPS L5 signal, the BDS B3I signal, and the Galileo E5a signal all adopt the modulation of BPSK(10) or the modulation that can be treated as BPSK(10) (European Union, 2013; China Satellite Navigation Office, 2018; Global Positioning Systems Directorate, 2018). Its power spectral density is given by (Kaplan and Hegarty, 2006):

$$
P_{BPSK}(f)=T_c\,\mathrm{sinc}^2(\pi f T_c) \tag{9}
$$

where T_c is defined as 1/10·23E6 (s). In the simulation, BPSK(10) is generated and filtered by the model shown in Figure 1. The generated filtered signal is further correlated with the replica codes for different correlator spacings; thus, the S-curves are obtained. By using the numerical method, the biases of the S-curves and the corresponding slopes for each of the given correlator spacings are calculated.

Figure 2 presents the comparisons of the theoretical and simulation results for different correlator spacings, and the results indicate that the theoretical results are in accord with the simulation results.

In Section 2, the original derived model includes the amplitude distortion of the channel. Here, to illuminate its impact on the slope, we add an amplitude distortion, which varies from −1 dB to 1 dB in the bandwidth linearly, to the filter model. The corresponding results in Figure 3 indicate that the addition of the amplitude distortion to the model described by the group delay in Figure 1 causes limited impacts on the slope distortion compared with the case of only existing group delay distortion.

https://doi.org/10.1017/S0373463321000035 Published online by Cambridge University Press

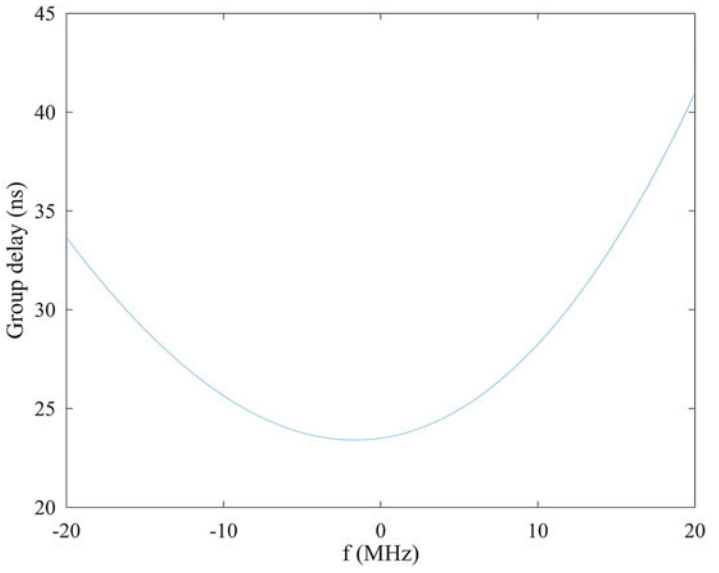

Figure 1. *Group delay used in the analysis and simulation.*

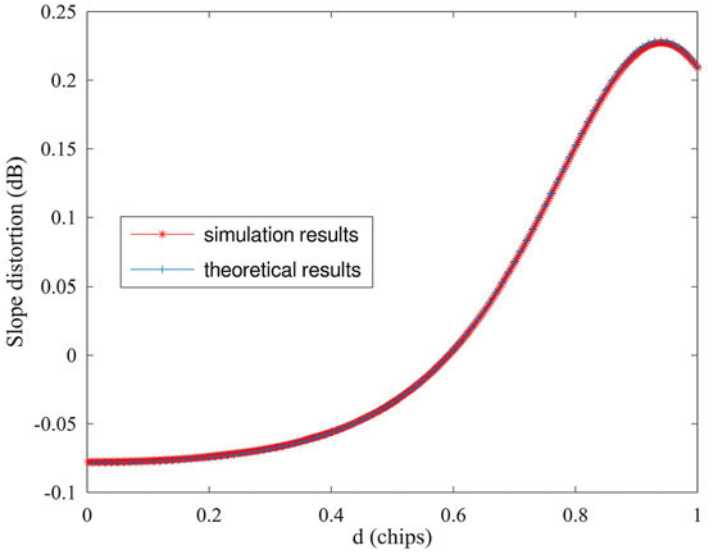

Figure 2. *Comparisons of the theoretical and simulation results.*

For clarity, we only consider the group delay in the model when analysing the slope distortion in the following sections, and then the frequency response of the filter becomes

$$H(f) = \mathrm{e}^{-\mathrm{i}*\theta(\mathrm{f})} \tag{10}$$

https://doi.org/10.1017/S0373463321000035 Published online by Cambridge University Press

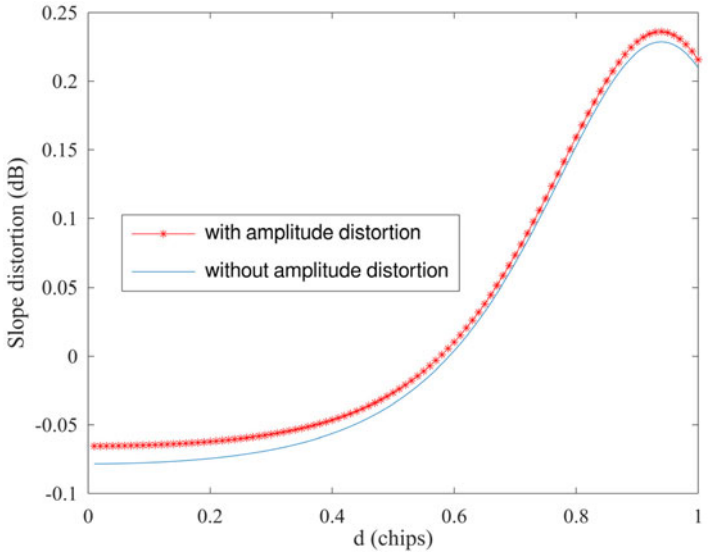

Figure 3. *Comparison of slope distortion between the cases with or without amplitude distortion.*

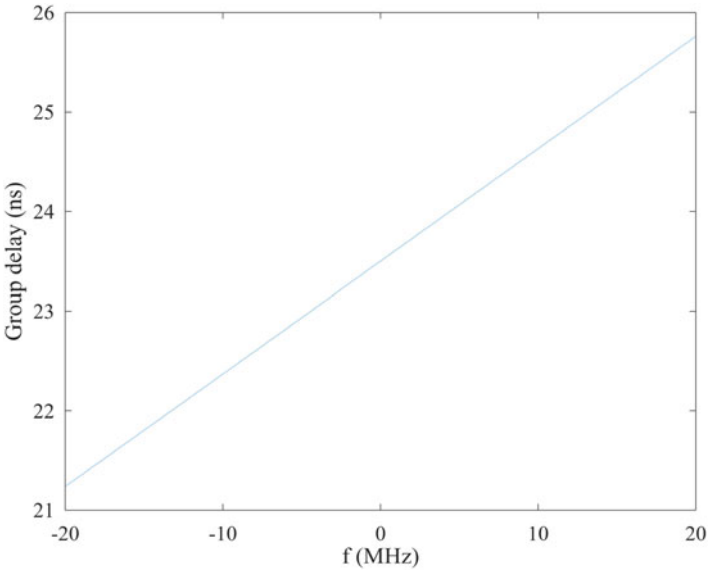

Figure 4. *Group delay within the bandwidth for the case of existing τ_g and τ_{g1} terms.*

4. Further analyses

4.1. Case A

In this case, $\theta(f) = \theta_0 - 2\pi\tau_g f$, and it is also the ideal case. The group delay is constantly equal to τ_g, and the filter delays all frequencies with the same amount. The signal passing through the filter is

https://doi.org/10.1017/S0373463321000035 Published online by Cambridge University Press

delayed by τ_g, thus $\tilde{\tau}$ is equal to τ_g. Applying $\tilde{\tau} = \tau_g$ to Equation (6) yields

$$K_{\mathrm{EMLP}}(d)|_{\tilde{\tau}=\tau_g} = 4P\mathrm{i}\pi \int_{-B_f/2}^{B_f/2} fP(f)e^{-\mathrm{i}d\pi f}\,\mathrm{d}f \int_{-B_f/2}^{B_f/2} P(f)e^{\mathrm{i}d\pi f T_c}\,\mathrm{d}f - 4P\mathrm{i}\pi \int_{-B_f/2}^{B_f/2} fP(f)e^{\mathrm{i}d\pi f}\,\mathrm{d}f \int_{-B_f/2}^{B_f/2} P(f)e^{-\mathrm{i}d\pi f}\,\mathrm{d}f \tag{11}$$

Further simplifying Equation (11) yields

$$K_{\mathrm{EMLP}}(d)|_{\tilde{\tau}=\tau_g} = 8P\pi \int_{-B_f/2}^{B_f/2} fP(f)\sin(d\pi fT_c)\mathrm{d}f \int_{-B_f/2}^{B_f/2} P(f)\cos(d\pi fT_c)\mathrm{d}f \tag{12}$$

In this case, $K_{\mathrm{EMLP}}^{\mathrm{ideal}}(d) = K_{\mathrm{EMLP}}(d)$ and $K_{sd}(d) = 0$.

4.2. Case B

In the case, the group delay contains the zeroth-order τ_g and the first-order τ_{g1} terms, then $\theta(f)$ is written as

$$\theta(f) = \theta_0 - 2\pi\tau_g f - \frac{1}{2}(2\pi)^2\tau_{g1}f^2 \tag{13}$$

For the properties of the odd-order terms (Liu et al., 2019), the delay $\tilde{\tau}$ due to the filter is equal to τ_g. Then, $K_{\mathrm{EMLP}}(d)|_{\tilde{\tau}=\tau_g}$ can be written as

$$\begin{aligned} K_{\mathrm{EMLP}}(d)|_{\tilde{\tau}=\tau_g} = {} & 2P\mathrm{i}\pi \int_{-B_f/2}^{B_f/2} fP(f)e^{-\mathrm{i}\frac{1}{2}(2\pi)^2\tau_{g1}f^2}e^{-\mathrm{i}\pi f\,dT_c}\mathrm{d}f \int_{-B_f/2}^{B_f/2} P(f)e^{\mathrm{i}\frac{1}{2}(2\pi)^2\tau_{g1}f^2}e^{\mathrm{i}\pi f\,dT_c}\mathrm{d}f \\ & - 2P\mathrm{i}\pi \int_{-B_f/2}^{B_f/2} fP(f)e^{\mathrm{i}\frac{1}{2}(2\pi)^2\tau_{g1}f^2}e^{\mathrm{i}\pi f\,dT_c}\mathrm{d}f \int_{-B_f/2}^{B_f/2} P(f)e^{-\mathrm{i}\frac{1}{2}(2\pi)^2\tau_{g1}f^2}e^{-\mathrm{i}\pi f\,dT_c}\mathrm{d}f \\ & - 2P\mathrm{i}\pi \int_{-B_f/2}^{B_f/2} fP(f)e^{-\mathrm{i}\frac{1}{2}(2\pi)^2\tau_{g1}f^2}e^{\mathrm{i}\pi f\,dT_c}\mathrm{d}f \int_{-B_f/2}^{B_f/2} P(f)e^{\mathrm{i}\frac{1}{2}(2\pi)^2\tau_{g1}f^2}e^{-\mathrm{i}\pi f\,dT_c}\mathrm{d}f \\ & + 2P\mathrm{i}\pi \int_{-B_f/2}^{B_f/2} fP(f)e^{\mathrm{i}\frac{1}{2}(2\pi)^2\tau_{g1}f^2}e^{-\mathrm{i}\pi f\,dT_c}\mathrm{d}f \int_{-B_f/2}^{B_f/2} P(f)e^{-\mathrm{i}\frac{1}{2}(2\pi)^2\tau_{g1}f^2}e^{\mathrm{i}\pi f\,dT_c}\mathrm{d}f \end{aligned} \tag{14}$$

Simplifying and rearranging Equation (14) yields

$$K_{\mathrm{EMLP}}(d)|_{\tilde{\tau}=\tau_g} = 4P\pi \left[\begin{array}{l} \displaystyle\int_{-B_f/2}^{B_f/2} fP(f)\cos(2\pi^2\tau_{g1}f^2)\sin(\pi f dT_c)\mathrm{d}f \\ \times \displaystyle\int_{-B_f/2}^{B_f/2} P(f)\cos(2\pi^2\tau_{g1}f^2)\cos(\pi f dT_c)\mathrm{d}f \\ + \displaystyle\int_{-B_f/2}^{B_f/2} fP(f)\sin(2\pi^2\tau_{g1}f^2)\sin(\pi f dT_c)\mathrm{d}f \\ \times \displaystyle\int_{-B_f/2}^{B_f/2} P(f)\sin(2\pi^2\tau_{g1}f^2)\cos(\pi f dT_c)\mathrm{d}f \end{array} \right] \tag{15}$$

https://doi.org/10.1017/S0373463321000035 Published online by Cambridge University Press

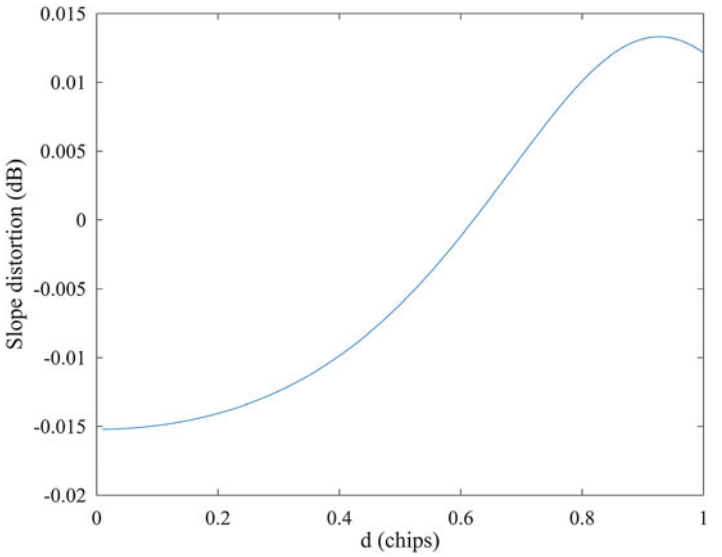

Figure 5. *Slope distortion versus correlator spacings for the case of existing τ_g and τ_{g1} terms.*

Substituting Equations (15) and (11) into (8) yields

$$K_{sd}(d) = \frac{\begin{bmatrix} \int_{-B_f/2}^{B_f/2} fP(f)\cos(2\pi^2\tau_{g1}f^2)\sin(\pi f dT_c)\mathrm{d}f \\ \times \int_{-B_f/2}^{B_f/2} P(f)\cos(2\pi^2\tau_{g1}f^2)\cos(\pi f dT_c)\mathrm{d}f \\ + \int_{-B_f/2}^{B_f/2} fP(f)\sin(2\pi^2\tau_{g1}f^2)\sin(\pi f dT_c)\mathrm{d}f \\ \times \int_{-B_f/2}^{B_f/2} P(f)\sin(2\pi^2\tau_{g1}f^2)\cos(\pi f dT_c)\mathrm{d}f \end{bmatrix}}{2\int_{-B_f/2}^{B_f/2} fP(f)\sin(\pi f dT_c)\mathrm{d}f \int_{-B_f/2}^{B_f/2} P(f)\cos(\pi f dT_c)\mathrm{d}f} \tag{16}$$

From the results shown in Equation (16), we can determine that the slope distortion is related to the first-order term, unlike the case for the bias. Since the group delay containing τ_g and τ_{g1} does not change the value of $D_{EMLP}(\tau_g)$ and does change the derivative of $D_{EMLP}(\tau_g)$, it has different impacts on the bias and slope of the S-curve.

Detailed analysis with the coefficients of $\tau_g = 23 \cdot 5\mathrm{E}-9$ (s) and $\tau_{g1} = 1 \cdot 8\mathrm{E}-17$ (s^2/rad) is performed in this case. The variation of group delay within the bandwidth in Figure 4 is 5 ns. Using Equation (16) with the given parameters of τ_g and τ_{g1}, we find that the slope distortion is less than 0·02 dB, as shown in Figure 5.

To further show the effect of the first-order term on the slope distortion in a more comparable case, we increase τ_{g1} to $5 \cdot 4\mathrm{E}-17$ (s^2/rad) to obtain the similar amount of the group delay fluctuation within the bandwidth caused by the second-order term in Section 4.3. As illustrated in Figures 6 and 7, the fluctuation of the group delay within the bandwidth enlarges to 15 ns, and the slope distortion for the worse case also increases to 0·15 dB.

4.3. Case C

For the case of the group delay composed of τ_g and τ_{g2} terms, $\theta(f)$ becomes

$$\theta(f) = \theta_0 - 2\pi\tau_g f - \frac{1}{6}(2\pi)^3\tau_{g2}f^3 \tag{17}$$

https://doi.org/10.1017/S0373463321000035 Published online by Cambridge University Press

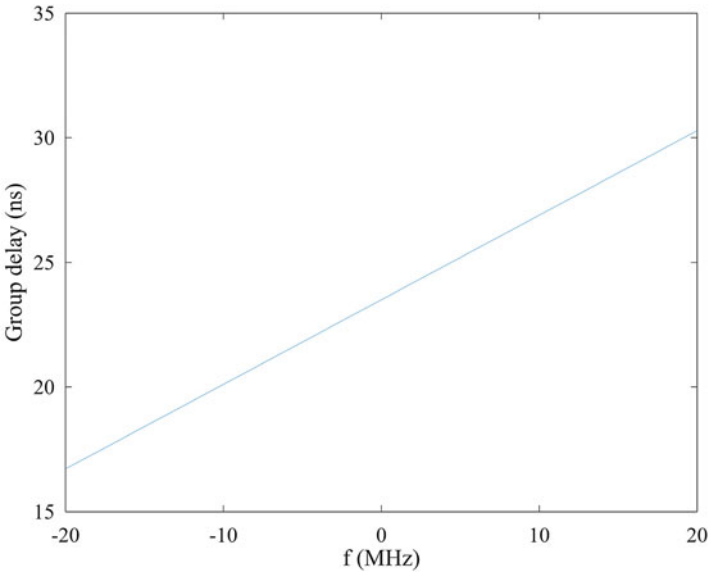

Figure 6. *Group delay within the bandwidth for the case of enlarged τ_{g1} term.*

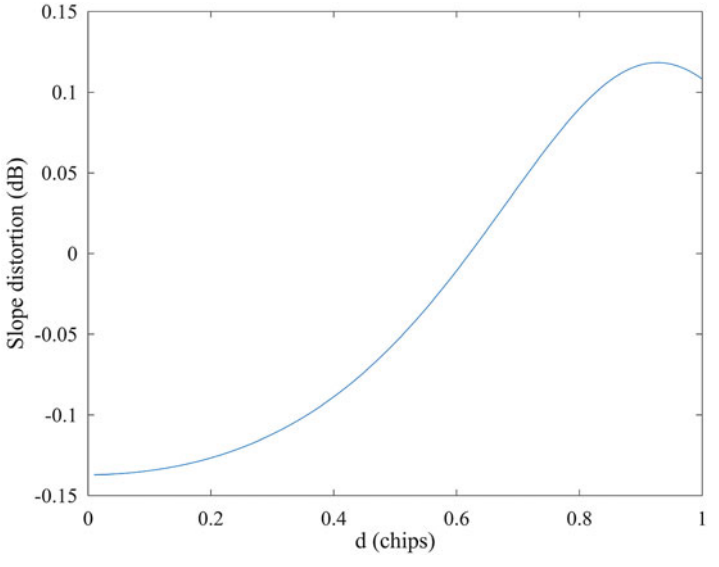

Figure 7. *Slope distortion versus correlator spacings for the case of enlarged τ_{g1} term.*

Due to the existence of the second-order terms, extra biases have been added to τ_g. Then, $\tilde{\tau}$ is given by

$$\tilde{\tau} = \tau_g + \Delta\tau + \delta\tau \tag{18}$$

The calculation of $\Delta\tau$ and $\delta\tau$ can be implemented by referring to Equations (4) and (5) in Section 2. Substituting Equation (18) into (3) and further simplifying the equation yields

$$K_{\mathrm{EMLP}}(d) = 4P\pi \int_{-B_f/2}^{B_f/2} fP(f) \sin\left(\frac{1}{6}(2\pi)^3\tau_{g2}f^3 - 2\pi f\left(\Delta\tau + \delta\tau - \frac{d}{2}T_c\right)\right)\mathrm{d}f$$
$$\times \int_{-B_f/2}^{B_f/2} P(f) \cos\left(\frac{1}{6}(2\pi)^3\tau_{g2}f^3 - 2\pi f\left(\Delta\tau + \delta\tau - \frac{d}{2}T_c\right)\right)\mathrm{d}f$$

https://doi.org/10.1017/S0373463321000035 Published online by Cambridge University Press

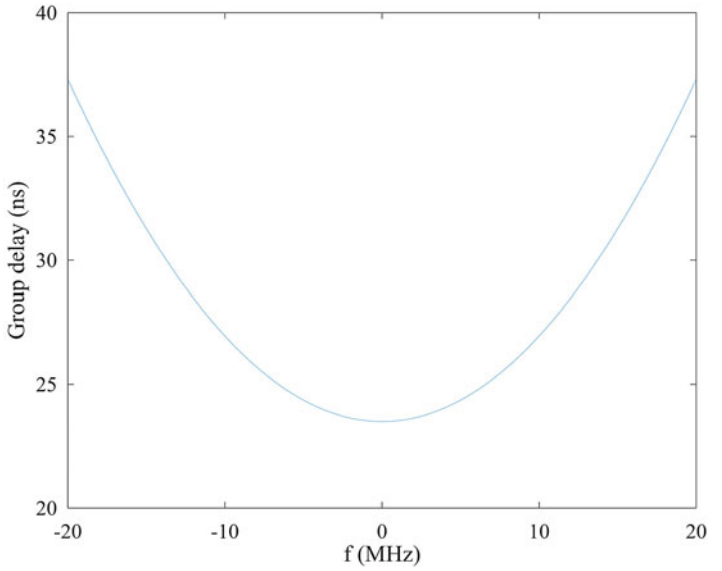

Figure 8. *Group delay within the bandwidth in the presence of τ_g and τ_{g2} terms.*

$$-4P\pi\int_{-B_f/2}^{B_f/2} fP(f)\sin\left(\frac{1}{6}(2\pi)^3\tau_{g2}f^3-2\pi f\left(\Delta\tau+\delta\tau+\frac{d}{2}T_c\right)\right)\mathrm{d}f$$
$$\times\int_{-B_f/2}^{B_f/2} P(f)\cos\left(\frac{1}{6}(2\pi)^3\tau_{g2}f^3-2\pi f\left(\Delta\tau+\delta\tau+\frac{d}{2}T_c\right)\right)\mathrm{d}f \tag{19}$$

Thus, $K_{sd}(d)$ is calculated as

$$K_{sd}(d)=\frac{\begin{array}{l}\int_{-B_f/2}^{B_f/2} fP(f)\sin\left(\frac{1}{6}(2\pi)^3\tau_{g2}f^3-2\pi f\left(\Delta\tau+\delta\tau-\frac{d}{2}T_c\right)\right)\mathrm{d}f\\ \times\int_{-B_f/2}^{B_f/2} P(f)\cos\left(\frac{1}{6}(2\pi)^3\tau_{g2}f^3-2\pi f\left(\Delta\tau+\delta\tau-\frac{d}{2}T_c\right)\right)\mathrm{d}f\\ -\int_{-B_f/2}^{B_f/2} fP(f)\sin\left(\frac{1}{6}(2\pi)^3\tau_{g2}f^3-2\pi f\left(\Delta\tau+\delta\tau+\frac{d}{2}T_c\right)\right)\mathrm{d}f\\ \times\int_{-B_f/2}^{B_f/2} P(f)\cos\left(\frac{1}{6}(2\pi)^3\tau_{g2}f^3-2\pi f\left(\Delta\tau+\delta\tau+\frac{d}{2}T_c\right)\right)\mathrm{d}f\end{array}}{2\int_{-B_f/2}^{B_f/2} fP(f)\sin(d\pi fT_c)\mathrm{d}f\int_{-B_f/2}^{B_f/2} P(f)\cos(d\pi fT_c)\mathrm{d}f} \tag{20}$$

Figure 8 presents the plot of the group delay determined by τ_g and τ_{g2} terms with the coefficients of $\tau_g = 23{\cdot}5\mathrm{E}{-}9$ (s) and $\tau_{g2} = 1{\cdot}75\mathrm{E}{-}24$ ($\mathrm{s}^3/\mathrm{rad}^2$). The results in Figure 8 show that the variation of the group delay is 15 ns, and the maximum of the corresponding slope distortion in Figure 9 is 0·23 dB. The result is slightly larger than the slope distortion with the enlarged first-order terms case in Section 4.2.

4.4. Case D

For this case, the group delay contains the zeroth-order and the third-order terms, and $\theta(f) = \theta_0 - 2\pi\tau_g f - \frac{1}{24}(2\pi)^4\tau_{g3}f^4$. For the characteristic of the odd-order term of group delay (Liu et al., 2019),

https://doi.org/10.1017/S0373463321000035 Published online by Cambridge University Press

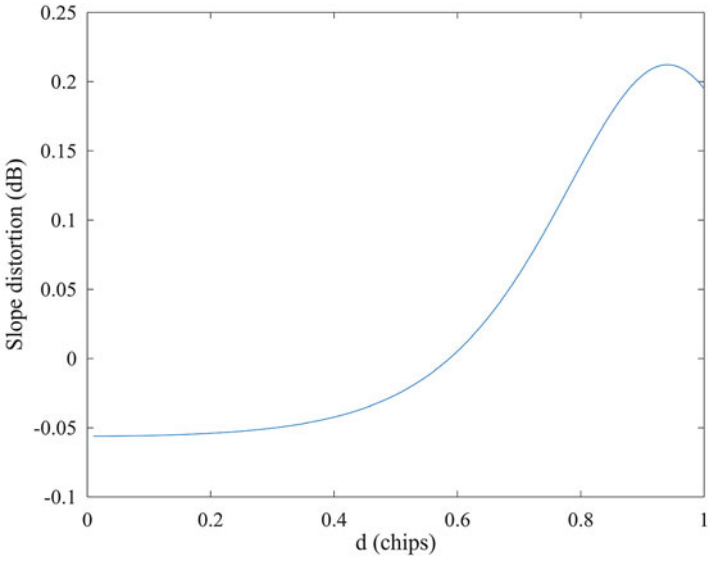

Figure 9. *Slope distortion versus correlator spacings in the presence τ_g and τ_{g1} terms.*

we can find that $\tilde{\tau} = \tau_g$. Then, the simplified expression can be expressed as

$$K_{\mathrm{EMLP}}(d) = 4P\pi \left[\begin{array}{l} \int_{-B_f/2}^{B_f/2} fP(f)\cos\left(\frac{1}{24}(2\pi)^4\tau_{g3}f^4\right)\sin(\pi f dT_c)\mathrm{d}f \\ \times \int_{-B_f/2}^{B_f/2} P(f)\cos\left(\frac{1}{24}(2\pi)^4\tau_{g3}f^4\right)\cos(\pi f dT_c)\mathrm{d}f \\ + \int_{-B_f/2}^{B_f/2} fP(f)\sin\left(\frac{1}{24}(2\pi)^4\tau_{g3}f^4\right)\sin(\pi f dT_c)\mathrm{d}f \\ \times \int_{-B_f/2}^{B_f/2} P(f)\sin\left(\frac{1}{24}(2\pi)^4\tau_{g3}f^4\right)\cos(\pi f dT_c)\mathrm{d}f \end{array} \right] \tag{21}$$

Substituting Equation (21) into (8) yields

$$K_{sd}(d) = \frac{\left[\begin{array}{l} \int_{-B_f/2}^{B_f/2} fP(f)\cos\left(\frac{1}{24}(2\pi)^4\tau_{g3}f^4\right)\sin(\pi f dT_c)\mathrm{d}f \\ \times \int_{-B_f/2}^{B_f/2} P(f)\cos\left(\frac{1}{24}(2\pi)^4\tau_{g3}f^4\right)\cos(\pi f dT_c)\mathrm{d}f \\ + \int_{-B_f/2}^{B_f/2} fP(f)\sin\left(\frac{1}{24}(2\pi)^4\tau_{g3}f^4\right)\sin(\pi f dT_c)\mathrm{d}f \\ \times \int_{-B_f/2}^{B_f/2} P(f)\sin\left(\frac{1}{24}(2\pi)^4\tau_{g3}f^4\right)\cos(\pi f dT_c)\mathrm{d}f \end{array} \right]}{2\int_{-B_f/2}^{B_f/2} fP(f)\sin(\pi f dT_c)\mathrm{d}f \int_{-B_f/2}^{B_f/2} P(f)\cos(\pi f dT_c)\mathrm{d}f} \tag{22}$$

Figure 10 shows the curve of the group delay with the coefficient of $\tau_{g3} = 4 \cdot 2\mathrm{E}-33$ $(\mathrm{s}^4/\mathrm{rad}^3)$. The variation of the group delay in this figure is 3 ns within the bandwidth, and the corresponding slope distortion is negligible, as shown in Figure 11.

https://doi.org/10.1017/S0373463321000035 Published online by Cambridge University Press

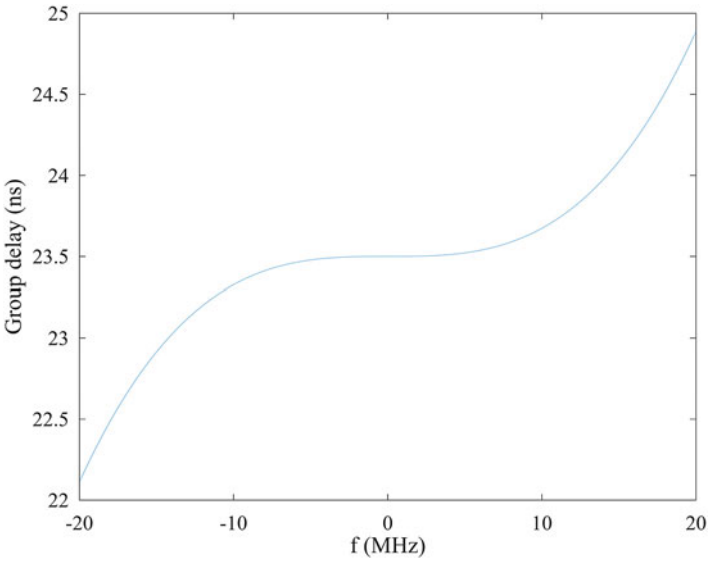

Figure 10. *Group delay within the bandwidth in the presence of τ_g and τ_{g3} terms.*

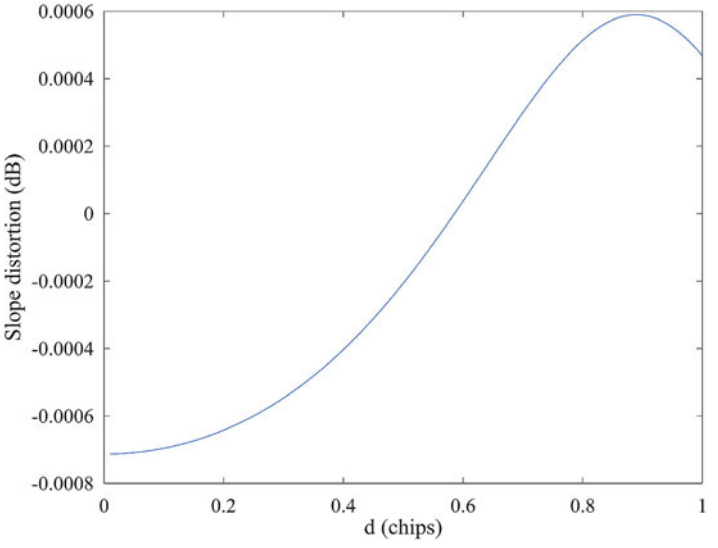

Figure 11. *Slope distortion versus correlator spacings in the presence τ_g and τ_{g3} terms.*

For comparisons among different cases in a similar range of variations of group delay, the third-order term τ_{g3} is increased to $2 \cdot 94\text{E} - 32$ $(\text{s}^4/\text{rad}^3)$. We can see that the fluctuation of the group delay in Figure 12 reaches 25 ns, and the slope distortion for this case in Figure 13 is less than 0·05 dB. Compared with the similar cases in Section 4.2 and Section 4.3, we find that the slope distortion affected by the terms of τ_g and τ_{g3} is much less than the other cases. This phenomenon is consistent with the shape of the group delay curve within the bandwidth. For the case of containing the terms of τ_g and τ_{g3}, the variation of the group delay as frequency limited to [−10 10] MHz, which corresponds to the main lode spectrum of the signal, is still limited. Due to the impact of the third power of frequency, more considerable variations of group delay concentrate on the margin of the frequency bandwidth.

https://doi.org/10.1017/S0373463321000035 Published online by Cambridge University Press

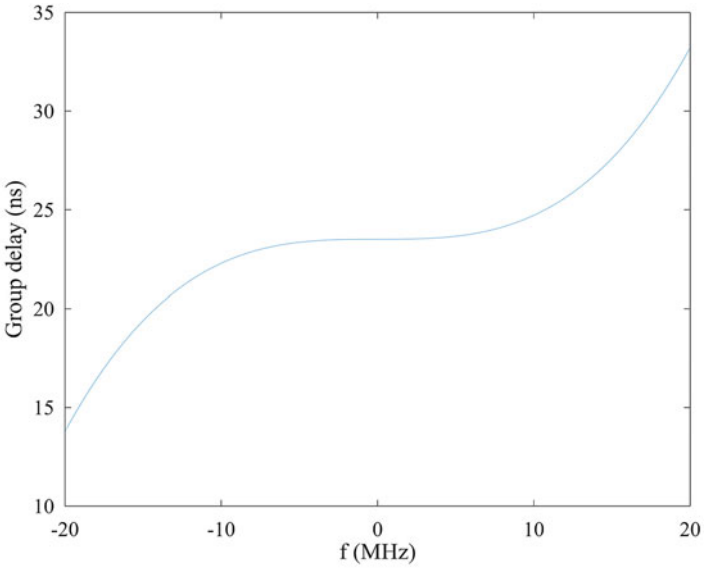

Figure 12. *Group delay within the bandwidth for the case of enlarged τ_{g3} term.*

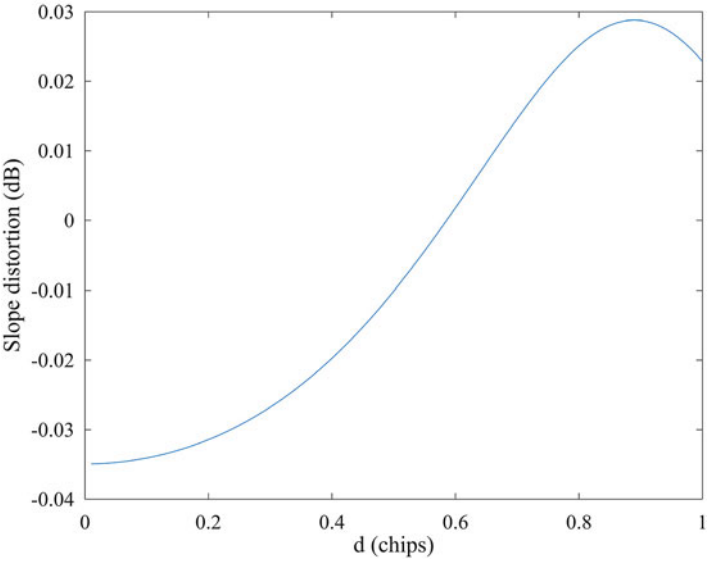

Figure 13. *Slope distortion versus correlator spacings for the case of enlarged τ_{g3} term.*

4.5. Case E

To compare the combined effect of more group delay terms on slope distortion, we calculate the slope distortions for the cases of (τ_g, τ_{g2}), (τ_g, τ_{g1}, τ_{g2}), and (τ_g, τ_{g1}, τ_{g2}, τ_{g3}). These coefficients are derived from the model in Section 2.

By using Equation (8), the slope distortions for the three cases are calculated and plotted in Figure 14. The results indicate that the addition of the term of τ_{g1} to the case shown in Section 4.3 causes little difference in the slope distortions. This phenomenon is because the slope distortion from the first-order term is very small, as shown in Section 4.2. Meanwhile, for the third-order term's limited impact on the slope distortion shown in Section 4.4, the addition of the term of τ_{g3} to the case containing the terms of τ_g, τ_{g1}, and τ_{g2} also brings little extra slope distortion.

https://doi.org/10.1017/S0373463321000035 Published online by Cambridge University Press

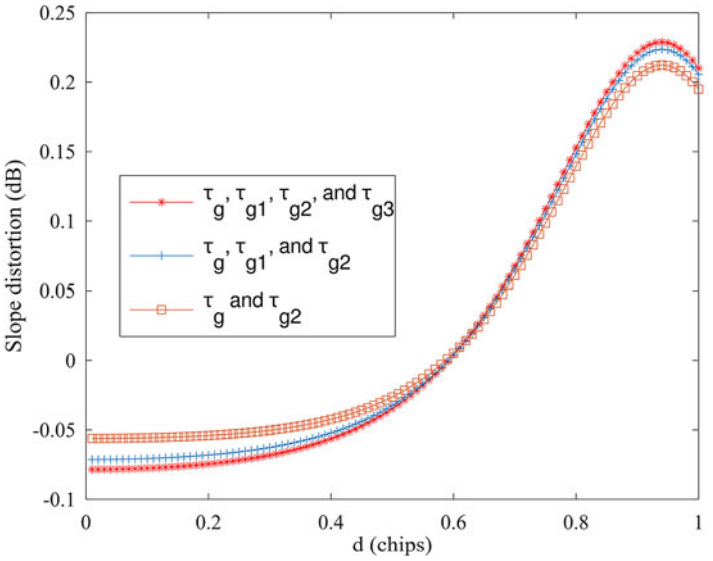

Figure 14. *Comparisons of slope distortions for different types of group delay composed of different order terms.*

4.6. Discussion

The optimisation of the RF channel for payloads or receivers to minimise the distortions of group delay is always an important issue. The shape of the group delay determined by different odd-order and even-order terms is related to the choice of the filter type, order and bandwidth. From the point of view of design, the selections of proper bandwidth and amount of out-of-band rejection of filters in the channel are helpful to decrease the fluctuation of group delay within the bandwidth. Too narrow bandwidth and larger suppression of adjacent out-of-band would cause more variation of group delay. Meanwhile, an equalisation network is another effective way to decrease the fluctuation of the group delay in the channel. The group delay of the equalisation network is designed to compensate for the fluctuation of the group delay of the channel. The cascade connection of the channel with the equalisation network would then show less variation of group delay.

5. Conclusion

The slope distortion of the discriminator curve has profound impacts on the performance of DLL under noise. To reduce the slope distortion due to the group delay from the transmitting or receiving channels, the slope distortions in the presence of several types of group delay terms are modelled and analysed theoretically. Based on the presented results, we find that both the odd- and even-orders terms of group delay have impacts on the slope distortion. The amplitude distortion has limited effect on the S-curve, and the higher odd-order terms of group delay cause fewer slope distortions under the same level of group delay fluctuation. The models and corresponding analysed results present a theoretical method of calculating the slope distortions derived from the group delay.

References

Betz, J. W. (2002). Effect of Linear Time-Invariant Distortions on RNSS Code Tracking Accuracy. *Proceedings of ION GPS 2002*, Institute of Navigation, Portland, OR, USA.

Betz, J. W. and Kolodziejski, K. R. (2009a). Generalized theory of code tracking with an early-late discriminator part I: Lower bound and coherent processing. *IEEE Transactions on Aerospace and Electronic Systems*, **45**, 1538–1556.

https://doi.org/10.1017/S0373463321000035 Published online by Cambridge University Press

Betz, J. W. and Kolodziejski, K. R. (2009b). Generalized theory of code tracking with an early-late discriminator part II: Noncoherent processing and numerical results. *IEEE Transactions on Aerospace and Electronic Systems*, **45**, 1557–1564.

China Satellite Navigation Office (2018). BeiDou Navigation Satellite System Signal in Space Interface Control Document Open Service Signal B3I (Version 1.0). Available at: http://beidou.gov.cn/xt/gfxz/201802/P020180209623601401189.pdf [Accessed 15 Dec. 2018].

European Union (2013). European GNSS (Galileo) open service signal in space interface control document. Available at: https://galileognss.eu/galileo-os-sis-icd/ [Accessed 15 Dec 2018].

Global Positioning Systems Directorate (2018). Navstar GPS Space Segment/User Segment L5 Interface. Available at: https://www.gps.gov/technical/icwg/. [Accessed 15 Dec 2018].

Gong, X., Lou, Y., Zheng, F., Gu, S., Shi, C., Liu, J. and Jing, G. (2018). Evaluation and calibration of BeiDou receiver-related pseudorange biases. *GPS Solutions*, **22**, 98.

Guo, N. Y., Kou, Y. H., Zhao, Y., Yu, Z. and Chen, Y. (2014). An all-pass filter for compensation of ionospheric dispersion effects on wideband GNSS signals. *GPS Solutions*, **18**, 625–637.

Hauschild, A. and Montenbruck, O. (2016). A study on the dependency of GNSS pseudorange biases on correlator spacing. *GPS Solutions*, **20**, 159–171.

He, C. Y., Lu, X. C., Guo, J., Su, C., Wang, W. and Wang, M. (2020). Initial analysis for characterizing and mitigating the pseudorange biases of BeiDou navigation satellite system. *Satellite Navigation*, **1**, 3.

Kaplan, E. and Hegarty, C. J. (2006). *Understanding GPS Principle*. Second edition. Norwood: Artech House.

Liu, Y. Q., Ran, Y. H., Ke, T. and Hu, X. L. (2012). Characterization of code tracking error of coherent DLL under CW interference. *Wireless. Personal. Communication*, **66**, 397–417.

Liu, Y. Q., Chen, L., Yang, Y., Pan, H. C. and Ran, Y. H. (2019). Theoretical evaluation of group delay on pseudorange bias. *GPS Solutions*, **23**, 69.

Liu, Y. Q., Yang, Y., Chen, L., Pan, H. C. and Ran, Y. H. (2020). Analysis of phase bias between GNSS signal components caused by non-ideal group delay. *Navigation*, **67**, 291–305.

Quan, Y., Lau, L., Roberts, G. W. and Meng, X. (2015). Measurement signal quality assessment on all available and new signals of multi-GNSS (GPS, GLONASS, Galileo, BDS, and QZSS) with real data. *The Journal of Navigation*, **69**(02), 313–334.

Soellner, M., Kohl, R., Luetke, W. and Erhard, P. (2002). The Impact of Linear and non-Linear Signal Distortions on Galileo Code Tracking Accuracy. *Proceedings of ION GPS 2002*, Institute of Navigation, Portland, OR, USA.

Thoelert, S., Steigenberger, P., Montenbruck, O. and Meurer, M. (2019). Signal analysis of the first GPS III satellite. *GPS Solutions*, **23**, 92.

Warner, E. S. and Last, J. D. (2009). Interpretation of S-curve and tracking error in a delay-lock-loop. *The Journal of Navigation*, **48**, 303–306.

Wu, W., Guo, F. and Zheng, J. (2020). Analysis of Galileo signal-in-space range error and positioning performance during 2015–2018. *Satellite Navigation*, **1**, 6.

Xie, J., Wang, H., Li, P. and Meng, Y. (2018). *Satellite Navigation System and Technology*. Beijing Institute of Technology Press, Beijing.

Yang, Y. X., Gao, W., Guo, S., Mao, Y. and Yang, Y. (2019). Introduction to BeiDou-3 navigation satellite system. *Navigation*, **66**, 7–18.

Yang, Y. X., Mao, Y. and Sun, B. (2020). Basic performance and future developments of BeiDou global navigation satellite system. *Satellite Navigation*, **1**, 1.

Zhu, X. W., Li, Y. L., Yon, S. W. and Zhuang, Z. W. (2009). A novel definition and measurement method of group delay and its application. *IEEE Transactions on Instrumentation and Measurement*, **58**, 229–233.

Cite this article: Liu Y, Ran Y, Yang Y, Chen L, Xiong T, Pan H (2021). Analysis of impact of group delay on slope distortion of S-curve in delay locked loop. *The Journal of Navigation* **74**: 3, 698–712. https://doi.org/10.1017/S0373463321000035